Two-layer mesoscopic modeling of bag break-up in turbulent secondary atomization

By N. Rimbert†, F. Doisneau‡¶, F. Laurent‡, D. Kah AND M. Massot‡

The secondary bag break-up mechanism is described and modeled at a mesoscopic scale using population balance equations as a first step towards industrial simulations of turbulent atomization. A stochastic process accounting for temporality and experimental asymptotics of turbulence-liquid interactions is built with a self similar kernel whereas larger droplets are only subject to a mean-flow-based discrete and instantaneous break-up kernel. For turbulence to influence only the small droplets, they are collected into a second population balance equation and renamed ligaments in relation with their transient shape during the process. The evolution of velocity distributions is introduced in the modeling as a driving parameter of the break-up process. Computations are made for William's full spray equation on simplified cases. Finally the model is reduced to a system of conservation equations in space and time with closed source terms thanks to the Eulerian Multi-Fluid approach, in order to be applicable for more realistic configurations.

1. Introduction

Turbulent atomization is of paramount importance for mechanical engineering where it typically requires simulation at a mesoscopic level, i.e., by disregarding the smallest scales. Indeed, Direct Numerical Simulations (DNS) of the liquid-gas interface are intractable for realistic Weber and Reynolds numbers. Even if DNS can give some insight and allow model validations, the development of numerical methods remains the main issue (Gorokhovski & Herrmann 2008; Le Chenadec 2012). As a result, Large Eddy Simulation (LES) seems to be the target level of description (Apte *et al.* 2003). The secondary stage of atomization - where droplets, which have been ripped off the dense core, break-up under the effect of surrounding turbulence - drives the final droplet size distribution so its mesoscopic modeling is the focal point of this contribution.

Turbulent atomization models are scarce and most experimentalists still resort to empirical number density functions (NDF) to describe the resulting size distribution of the droplet mist (Lefebvre 1989). Such NDFs can be directly used to close secondary break-up sources in Population Balance Equations (PBE) (Amsden *et al.* 1989); these equations can be generalized to transport and approached by moment methods (Dufour *et al.* 2003; Doisneau *et al.* 2013; Doisneau 2013). All these mesoscopic models using presumed NDFs are still popular but, by abandoning all the break-up timescales, they lack temporality. Also, the instantaneous velocity jump from the mother to the daughter droplets, using low-definition empirical laws, is of limited accuracy and brings in numerical convergence issues. Hence a mechanism, even simple, is required to bridge the gap between a micro-

† LEMTA, ESSTIN, Université de Lorraine
‡ Département d'Énergétique Fondamentale et Appliquée (DEFA), ONERA
¶ Laboratoire EM2C, UPR 288 CNRS and École Centrale Paris

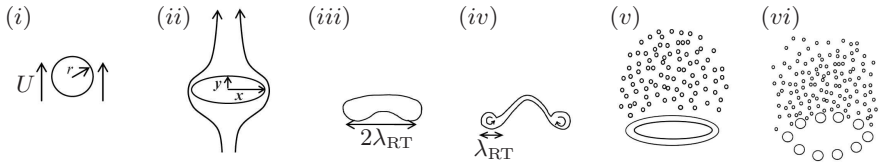

FIGURE 1. The six stages of bag break-up.

scopic DNS description and the target mesoscopic models in order to properly describe the spray size and velocity distributions.

The huge range of scales in turbulent sprays was early modeled as log-normal, which led eventually Kolmogorov (1941) to devise a stochastic process explaining their widespread appearance. This modeling became famous when used later to describe turbulence intermittencies (between large and small vortices, see Rimbert 2010 for more details). However, when the liquid jet flows rather slowly, classical linear instabilities are well known to govern the mechanism of drop formation and lead to narrow-band spectra. These two visions should therefore be merged into a comprehensive theory, based on a consistent description level: ligaments - which have been detected as soon as high-speed imaging became available in the late stage of the atomization process (Pilch & Erdman 1987) - are good candidates as either produced by cascading eddies or subject to capillary instabilities. These two visions are partially mapped by Eggers & Villermaux (2008), as far as linear instabilities and ligament reorganization into spherical droplets are concerned, and by Gorokhovski & Herrmann (2008) as far as Kolmogorov theory is concerned. In recent work Rimbert & Castanet (2011) attempted such an alliance to explain the experimental classification of secondary break-up made by Faeth's Group in Ann Arbor (Hsiang & Faeth 1995) as well as experimental NDF tails.

In the present work, a mechanism is built through a PBE combining discrete and self-similar break-up kernels: the process' asymptotic distribution matches an experimental NDF while its temporality is based on timescales from classical physical analysis. For the sake of clarity we focus on bag break-up, whose asymptotics is a Log-Lévy distribution (a generalization of log-normal laws). The so-forged mechanism is then extended by considering two PBEs in order to separately account for transient ligaments (mostly reorganized by turbulent-surface-tension competition) and for spherical droplets (assumed to be mostly insensitive to turbulence). This leads to a two-layer mesoscopic model which describes a different physics for droplets (discrete break-up) and ligaments (self-similar turbulent reorganization). The role of droplet velocities is then included so that each PBE is generalized into a kinetic equation referred to as GPBE and classically used for the LES of disperse phase flows (Fox 2012). Finally, the compliance of the overall modeling with state-of-the-art moment methods (Massot *et al.* 2009) is assessed.

2. A forged bag break-up process for temporality and asymptotics

2.1. *Bag breakup phenomenology*

The non-dimensional parameters that govern the stability of a droplet in a gas stream are the (aerodynamic) Weber number and the Ohnesorge number defined by $\mathrm{We} = \rho_g U^2 d/\sigma$, $\mathrm{Oh} = \mu_l/\sqrt{\sigma \rho_\mathrm{l} d}$ where ρ_g and ρ_l stand respectively for the gas and the liquid density, σ is the surface tension, μ_l is the liquid dynamic viscosity, d the droplet diameter and U the relative velocity between droplets and the gas. Using these two parameters Faeth and co-workers made a thorough investigation of the different kinds of atomization

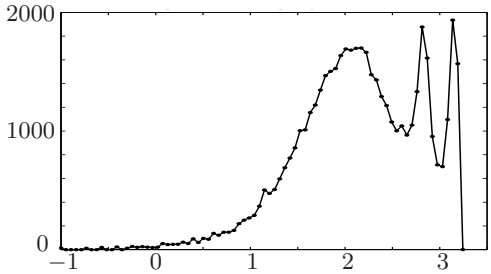

FIGURE 2. Experimental NDF of bag break-up – size in decimal magnitude, 0 stands for 1μm.

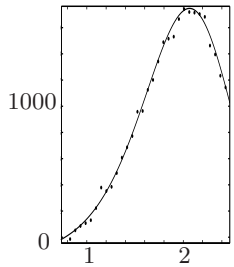

FIGURE 3. Experimental NDF tail (bag mode) fitted by a log-Lévy law ($\alpha = 1.69$).

mechanisms (Pilch & Erdman 1987) : elongation, bag break-up, umbrella break-up, shear break-up, etc., resulting in a We-Oh map classifying these phenomena (Hsiang & Faeth 1995). For simplicity, we focus on bag break-up as the lowest-speed break-up regime experimentally listed, and as mostly represented in secondary atomization cascades.

The bag break-up is usually decomposed into six stages shown in Figure 1 and its temporality is governed by the Rangers & Nichols characteristic time τ_{RN} which describes gas-liquid momentum exchanges (Hsiang & Faeth 1995). The Rayleigh-Taylor length λ_{RT} drives the rim size as the corresponding instability settles in steps (iii) and (iv). The bag breaks at step (v) after $3\tau_{\mathrm{RN}}$ and the rim disrupts at step (vi) after $5\tau_{\mathrm{RN}}$, concluding the break-up process so that a characteristic frequency linked to its total duration follows:

$$\nu = \frac{1}{5\tau_{\mathrm{RN}}} = \sqrt{\frac{\rho_g}{\rho_{\mathrm{l}}}}\frac{U}{5d}. \tag{2.1}$$

We assume the Weber range for bag break-up to be between $\mathrm{We}_b^- = 12$ and $\mathrm{We}_b^+ = 50$ and the parting of the liquid into the rim and the bag to be (R_d,R_l)=(75%, 25%). Radii of the droplets obtained from the break-up of the rim are assumed to be half the radius of the mother droplet - though it could be obtained from other considerations (Zhao *et al.* 2010). These considerations of volume branching ratio and rim droplet sizes will be used to build the rim-break-up kernel. One of the important results of Rimbert & Castanet (2011) is that, in the bag break-up regime, the small size droplet NDF tail can be adequately fitted by a log-stable Lévy law, an extension of log-normal laws. Figure 2 depicts the whole NDF and three modes are identified, from right to left: the mother droplet peak, the rim droplet peak and a wider mode of small size droplets resulting from the bag breakage. Figure 3 shows the fitting of the small size NDF by a log-stable law.

Though log-stable laws were first proposed for turbulent sprays by Novikov & Dommermuth (1997) and then by Rimbert & Séro-Guillaume (2004*b*), the main advance of the two papers Rimbert (2010) and Rimbert & Castanet (2011) is to give a physical interpretation to the parameters of the law e.g. stability index, scale parameter. It is therefore possible to cease considering them as fitting parameters. The stability index $\alpha = 1.70$ is related to a model of intermittency based on Self-Avoiding Vortex Random Stretching while the scale and shift parameters are related to the Kolmogorov and Taylor scale of the turbulence through a ligament turbulent reorganization mechanism. The size of the smallest drops is comparable to the Kolmogorov scale $\eta \approx 3\mu m$ and the size of the average drop compares to the estimated Taylor scale $\lambda \approx 137\mu m$. The width of the distribution has been estimated to be $\sigma_{\ln(d)} = 1/2\ln(\lambda/\eta)^{1/\alpha}$.

2.2. *A new process for break-up PBEs*

In the bag break-up regime, a droplet breaks into two classes of daughter droplets which are taken of equal size as a first approximation. Though the process is somewhat discontinuous (*cf.* the six stages reported in Figure 1), it is possible to write a continuous-in-time break-up equation by making the balance between the number of parent and daughter drops in a statistical sense. When the parents generate a single class of γ daughter droplets of equal radius $r_\gamma = r/\gamma^{\frac{1}{3}}$ with a frequency ν, the break-up equation reads

$$\frac{\partial f}{\partial t}(r) = -\nu f(r) + \int_{\mathbb{R}^+} \nu f(r')\gamma\delta_{r_\gamma}(r')\mathrm{d}r', \tag{2.2}$$

where $f(t,r)$ is the NDF of droplets of radius r per unit volume and δ_{r_γ} is Dirac's delta function centered on r_γ. An alternate way of writing the break-up equation is to use a self-similar form (Gorokhovski & Saveliev 2003):

$$\frac{\partial f}{\partial t}(r) = -\nu f(r) + \int_{\mathbb{R}^+} \nu f(r') b(r'/r)\mathrm{d}r'/r', \tag{2.3}$$

where b is the self-similar break-up kernel (most of the time unknown in real applications). Under appropriate hypotheses, the asymptotic behavior of Eq. (2.3) is a log-normal NDF therefore relating it to some turbulence cascading mechanism. However, in order to obtain a log-stable law and match experimental results, the kernel must be in the corresponding attraction basin which is roughly equivalent to the following asymptotic behavior:

$$b(r/r') \approx \frac{1}{|\ln(r'/r)|^{\alpha+1}}, \tag{2.4}$$

where α is the stability index of the Lévy law. To prevent divergence of integrals, we may either limit this kernel (e.g., truncate) or introduce a constant K_1 such that:

$$\frac{\partial f}{\partial t}(r) = -\nu f(r) + K_0 \int_{\mathbb{R}^+} \nu f(r') \frac{1}{|\ln(r'/r)|^{\alpha+1}}\mathrm{d}r'/r' + K_1 r \frac{\partial f}{\partial r}(r), \tag{2.5}$$

where K_0 is a constant governing the influence of the turbulent peak broadening and K_1 is a constant computed to enforce volume conservation. Although using Eq. (2.5) over Eq. (2.3) combined to a limited form of Eq. (2.4) somewhat changes the time dynamics (Eq. (2.4) leads to a log-stable law asymptotically while Eq. (2.5) leads to it instantaneously), it does not change the modeling qualitatively and has been chosen in the present work for numerical reasons. In the $\xi = \log_{10}(r)$ space or magnitude space Eq. (2.5) turns to

$$\frac{\partial f}{\partial t}(\xi) = -\nu f(\xi) + K_0 \int_{\mathbb{R}} \nu f(\xi') \frac{1}{|\xi' - \xi|^{\alpha+1}}\mathrm{d}\xi' + K_1 \frac{\partial f}{\partial \xi}(\xi) \tag{2.6}$$

Note that ν can have a variable value when updating U and d, leading to an increasing frequency as the droplet size decreases, yielding an infinite number of infinitely small particles in a finite time. This is referred to as shattering transition (Ziff & McGrady 1987) and is physically not desirable here so we choose a constant frequency based on the mother droplet size and velocity. Using Weyl's fractional derivative, expressed as follows:

$$\boldsymbol{D}^\alpha_\xi f(\xi) = \frac{1}{\Gamma(2-\alpha)} \frac{\partial^2}{\partial \xi^2} \int_{\mathbb{R}} f(\xi') \frac{1}{|\xi' - \xi|^{\alpha-1}}\mathrm{d}\xi', \tag{2.7}$$

Eq. (2.6) becomes formally a Fractional Fokker-Planck Equation, for a scale diffusion stochastic process, or can be seen as the generator of the approriate Lévy-Feller semigroup

(Rimbert & Séro-Guillaume 2004*a*), and reads:

$$\frac{\partial f}{\partial t}(\xi) = -\nu f(\xi) + \nu\chi_\alpha \boldsymbol{D}_\xi^\alpha f(\xi) + K_2 \frac{\partial f}{\partial \xi}(\xi), \tag{2.8}$$

where χ_α stands for $\sigma^\alpha cos(\pi\alpha/2)$ and is roughly equal to unity in our case (and replaces constant K_0). As integro-differential operators in Eq. (2.5) and Eq. (2.7) are proportional (this can be seen using a Fourier transform), constant K_2 replaces K_1 and must be set equal to $\nu\chi_\alpha(4^\alpha\Gamma(-\alpha)-1)/4$ to ensure volume conservation.

We finally have a discrete, i.e., instantaneous process (2.2), which we will use to model the rim break-up and the formation of the ligaments from the bag and a continuous process (2.8) which we will use to model the broadening of the ligament mode, presumably in relation with turbulence.

3. Two-layer mesoscopic models for droplets and ligaments

3.1. *Two-layer PBE model for droplets and ligaments*

If one considers an initial droplet submitted to Eq. (2.2), a cascading mechanism naturally occurs as the daughter droplets will themselves be divided into p fragments. It is not the case in the bag break-up mechanism, mostly because the relative velocity of the daughter drops and the surrounding gas is strongly decreasing during the process. A way to prevent daughter structures from breaking-up with the same mechanism is to separate bag structures into a second population called ligaments. We now use an index $p\in\{d,l\}$ for each population with d referring to droplets and l to ligaments. So the mother droplets breakup into two classes: the rim droplets whose volume ratio is $\gamma_d = 2^3$ according to experimental observations (Rimbert & Castanet 2011), and the bag ligaments whose volume ratio is given by $\gamma_l = 7^3$. Then the bag ligaments are affected by turbulent re-agglomeration and subject to process (2.8). Ligaments are supposed to be fully described by an equivalent diameter when assuming a 1D parametrization of their shape. Though a 2D manifold is required to render at least spheroidal (or cylindrical) shapes, this information was not measured by Rimbert & Castanet (2011) and is not included in the present model for the sake of simplicity. It is therefore of capital importance to presume the topologies of droplets and ligaments for size ξ and for each population p to compute the geometric features that are volumes $\mathcal{V}_p(\xi)$, surfaces $\mathrm{Surf}_p(\xi)$, etc. The Population Balance Equations (PBE) on $f_d(\xi)$ and $f_l(\xi)$ finally read:

$$\frac{\partial f_d}{\partial t} = -\nu_d f_d + R_d \int_{\mathbb{R}} \nu_d f_d(\xi') b_d(\xi',\xi)\mathrm{d}\xi' + \mathscr{C}^{ld+}(f_l), \tag{3.1}$$

$$\frac{\partial f_l}{\partial t} = R_l \int_{\mathbb{R}} \nu_d f_d(\xi') b_l(\xi',\xi)\mathrm{d}\xi' - \nu_l f_l + \nu_l\chi_\alpha \boldsymbol{D}_\xi^\alpha f_l(\xi) + K_2 \frac{\partial f_l}{\partial \xi} - \mathscr{C}^{ld-}(f_l), \tag{3.2}$$

where the kernels are noted $b_p = \gamma_p \delta_{\xi_p}(\xi')$ with $\xi_p = \xi - \frac{1}{3}\log_{10}(\gamma_p)$, $\nu_d = 5\tau_{\mathrm{RN}}\mathbf{1}_{[\mathrm{We}_b^-,\mathrm{We}_b^+]}$, $\nu_l = 5\tau_{\mathrm{RN}}\mathbf{1}_{[\mathrm{We}_b^-,\mathrm{We}_b^+]}$ and $\mathbf{1}_{[\mathrm{We}_b^-,\mathrm{We}_b^+]}\big(\mathrm{We}(\xi')\big)$ the characteristic function of the bag break-up domain. The two PBEs are coupled through the discrete break-up creation terms and through the sources $\mathscr{C}^{ld\pm}(f_l)$. The $\mathscr{C}^{ld\pm}$ terms translate the ligaments back to the droplet population once they have reordered, presumably under capillary forces:

$$\mathscr{C}^{ld-} = \nu_c f_l(\xi)\mathbf{1}_{\xi<\xi_0}(\xi) \text{ and } \mathscr{C}^{ld+} = \int_{-\infty}^{\xi_0} \nu_c f_l(\xi') c_l(\xi',\xi)\mathrm{d}\xi' \tag{3.3}$$

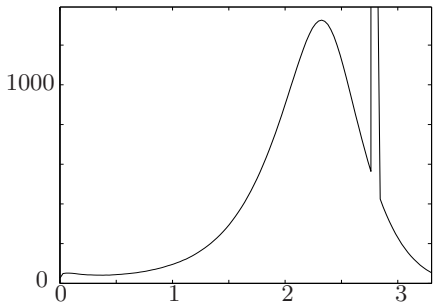

FIGURE 4. Spray NDF with the Two-Layer PBE model.

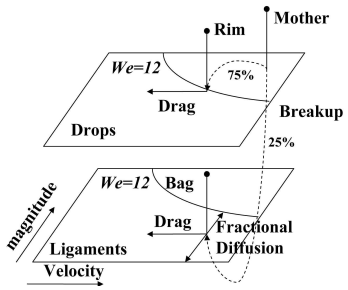

FIGURE 5. Scheme of the two layers containing drops (top) and ligaments (bottom).

with the frequency ν_c linked to the capillary number and the capillary reorganization kernel given by $c_l = \delta_{\mathcal{V}_l(\xi')}\big(\mathcal{V}_d(\xi)\big)$. The overall system, referred to as a Two-Layer PBE model, is conservative since:

- the droplet disappearance term $-\nu_d f_d$ is exactly balanced by the (rim) droplet and (bag) ligament discrete creation terms thanks to the branching relation $R_l + R_d = 1$;
- the continuous self-similar break-up process is mass conserving by construction;
- the capillary transfer sources ensure $\int_{\mathbb{R}}\mathcal{V}_l(\xi)\mathscr{C}^{ld-}(f_l(\xi))\mathrm{d}\xi = \int_{\mathbb{R}}\mathcal{V}_d(\xi')\mathscr{C}^{ld+}(f_l(\xi),\xi')\mathrm{d}\xi'$.

We now perform a simulation of the Two-Layer PBE model. A discretization of Eq. (3.2) is done analogously to Rimbert & Séro-Guillaume (2004*a*) using the algorithm of Gorenflo *et al.* (2002) for the fractional derivative. We take initial magnitudes of 3.13 ($1350\mu m$), initial velocities of 41m/s and initial Weber numbers of 41 for the mother droplets. In order to prevent subsequent (and spurious) break-up of the daughter rim droplets ($\mathrm{We}_{\mathrm{rim}} = 20.5$), We_b^- has been increased to the value of 23, theoretically derived by Rimbert & Castanet (2011). The resulting NDF is depicted in Figure 4. Note that the mother droplet is not shown on this picture as it has fully disappeared at the end of this atomization process. Since the terms $\mathscr{C}^{ld\pm}$ are not further modeled (ν_c has yet to be determined), they are not considered here and a zero flux boundary condition is imposed instead on the lower end of the magnitude (size) space, in order to prevent the appearance of very small ligaments. This uses the so-called image method (Gorenflo *et al.* 2002) and ensures mass conservation of the ligaments. The result corresponds to the superposition of the rim droplet peak to the wide ligament mode. If the simulation is left running further there will be an unphysical increase of small droplets on the lower size boundary. So the diffusion process must be stopped adequately, e.g., by introducing the terms $\mathscr{C}^{ld\pm}$ to transfer ligaments to the droplet space. Such terms are physically sound as a capillary reformation of droplets and should include the corresponding time scale, but their exact form is left for future work.

3.2. *Accounting for deceleration: two-layer GPBE model*

To refine the model and cope with the problem of daughter droplet stability more physically, we include the positions $\mathbf{x}$ and velocities $\mathbf{c}$ in the phase space, leading to Generalized PBEs or GPBEs (Williams 1958). Since Weber numbers depend on $\mathbf{c}$, break-up processes are now conditioned on velocities. This results in the Two-Layer GPBE model on $f_p(\xi,\mathbf{c})$:

$$\frac{\partial f_d}{\partial t} + \mathbf{c}\frac{\partial f_d}{\partial \mathbf{x}} + \frac{\partial \mathbf{a}_d f_d}{\partial \mathbf{c}} = -\nu_d f_d + R_d \iint_{\mathbb{R}^2} \nu_d f_d(\xi',\mathbf{c}') b_d(\xi',\mathbf{c}',\xi)\beta_d(\xi',\mathbf{c}',\mathbf{c})\mathrm{d}\xi'\mathrm{d}\mathbf{c}' + \mathscr{C}^{ld+}(f_l) \quad (3.4)$$

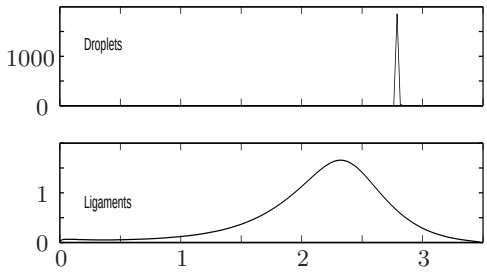

FIGURE 6. NDF of droplets and of ligaments with the Two-Layer GPBE model.

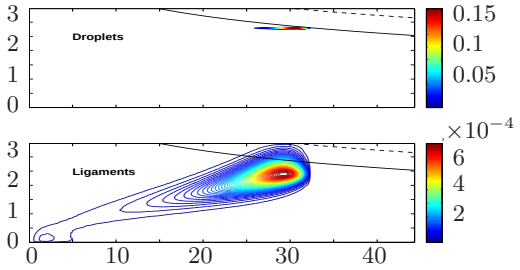

FIGURE 7. NDF in magnitude-velocity space. Dotted and solid line limit $\mathrm{We}_b^- < \mathrm{We} < \mathrm{We}_b^+$.

$$\begin{aligned}\frac{\partial f_l}{\partial t} + \mathbf{c}\frac{\partial f_l}{\partial \mathbf{x}} + \frac{\partial \mathbf{a}_l f_l}{\partial \mathbf{c}} = \quad & R_l \iint_{\mathbb{R}^2} \nu_d f_d(\xi', \mathbf{c}') b_l(\xi', \mathbf{c}', \xi) \beta_l(\xi', \mathbf{c}', \mathbf{c}) \mathrm{d}\xi' \mathrm{d}\mathbf{c}' \\ & -\nu_l f_l + \chi_\alpha \boldsymbol{D}_\xi^\alpha f_l + K_2 \frac{\partial f_l}{\partial \xi} - \mathscr{C}^{ld-}(f_l);\end{aligned} \tag{3.5}$$

The accelerations $\mathbf{a}_p(\mathbf{c}, \xi)$ depend in general on the droplet shape ξ and the relative velocity $\mathbf{c}$. For the sake of simplicity, the velocity kernels are taken to be monokinetic ,i.e., with a zero dispersion $\beta_p = \delta\big(\mathbf{c} - \mathbf{u}_p^{\mathrm{B}}\big)$ and the target relative velocity $\mathbf{u}_p^{\mathrm{B}}(\xi', \mathbf{c}')$ is computed from the mother droplet so that the rim droplets have a Weber number slightly below We_b^- to stop the breakage. Note that the spurious succeeding cascade of fragmentation of Section 3.1 are naturally eliminated in this process. We highlight that the choice of $\mathbf{u}_p^{\mathrm{B}}$ models the integral effect of drag during the discrete break-up process; it therefore requires a counterpart term for the the carrier phase equations to enforce momentum conservation in a two-way coupling context. A schematic description of the overall liquid behavior in the two-layer phase space can be found in Figure 5.

The spray break-up is now computed with the Two-Layer GPBE model with the same initial conditions as previously. Because such kinetic equations have a prohibitive cost, we remove the physical space dependence on $\mathbf{x}$ by considering the problem to be homogeneous in space by analogy with well-stirred reactor hypotheses in chemistry. Moreover the velocity is in 1D. We take for the sake of simplicity $\mathbf{a}_p = \mathbf{g} - \rho_{\mathrm{l}} \mathrm{Surf}(\xi) C_d |\mathbf{c}| \mathbf{c}$ with $C_d = 1.0$ for both droplets and ligaments, $\mathbf{g}$ stands for the gravity. Results after $5\tau_{\mathrm{RN}}$ are given for the NDF in Figure 6 and the behavior in phase space can be found in Figure 7. The shape of the experimental NDF in Figure 2 is again recovered according to the *ad hoc* choice of the stochastic process.

4. Towards CFD codes: discussion on moment methods for model reduction

The Two-Layer GPBE model has been computed with a 0D physical and 1D velocity space for cost-cutting reasons but the full picture is heterogeneous and 3D. The purpose of this section is to show how to reduce the full model to a set of conservation equations on the physical space for the approach to be easily included into CFD softwares ,e.g., for diesel injection (Kah 2010) or solid rocket motors (Doisneau *et al.* 2013; Doisneau 2013).

4.1. *Velocity moment method: the semi-kinetic model*

In a first step we reduce the Two-Layer GPBE phase spaces to the only droplet size variable. We consider velocity moments that are the number density $n_p = \int_{\mathbb{R}} f_p(\xi, \mathbf{c}) \mathrm{d}\mathbf{c}$ and the average momentum $n_p \mathbf{u}_p = \int_{\mathbb{R}} \mathbf{c} f_p(\xi, \mathbf{c}) \mathrm{d}\mathbf{c}$. In order to close the system, the

NDFs are approximated according to a monokinetic hypothesis:

$$f_p(\xi, \mathbf{c}) = n_p(\xi)\delta(\mathbf{c} - \mathbf{u}_p), \tag{4.1}$$

which means that for a given size ξ and location $(t, \mathbf{x})$, the only characteristic velocity is the average $\mathbf{u}_p(t, \mathbf{x}, \xi)$ while the velocity dispersion around $\mathbf{u}_p(t, \mathbf{x}, \xi)$ is zero in each direction. This assumption is correct when the drag force characteristic time is small compared to the local gas characteristic dynamic time (Massot *et al.* 2009). This step leads to two systems of conservation equations called semi-kinetic, which read:

$$\left\{\begin{array}{ll} \partial_t n_d + \partial_{\mathbf{x}} \cdot (n_d \mathbf{u}_d) & = -\mathscr{B}^{n_d -} + \mathscr{B}^{n_d d+} + \mathscr{C}^{n_l d+} \\ \partial_t (n_d \mathbf{u}_d) + \partial_{\mathbf{x}} \cdot (n_d \mathbf{u}_d \otimes \mathbf{u}_d) & = -\mathscr{B}^{u_d -} + \mathscr{B}^{u_d d+} + \mathscr{C}^{u_l d+} + n_d \overline{\mathbf{a}}_d \end{array}\right. \tag{4.2}$$

$$\left\{\begin{array}{ll} \partial_t n_l + \partial_{\mathbf{x}} \cdot (n_l \mathbf{u}_l) & = \mathscr{B}^{n_d l+} - \mathscr{B}^{n_l -} + \mathscr{B}^{n_l l+} - \mathscr{C}^{n_l d-} \\ \partial_t (n_l \mathbf{u}_l) + \partial_{\mathbf{x}} \cdot (n_l \mathbf{u}_l \otimes \mathbf{u}_l) & = \mathscr{B}^{u_d l+} - \mathscr{B}^{u_l -} + \mathscr{B}^{u_l l+} - \mathscr{C}^{u_l d-} + n_l \overline{\mathbf{a}}_l \end{array}\right. \tag{4.3}$$

where one gets, still with $p \in \{d, l\}$, the average acceleration $n\overline{\mathbf{a}}_p = \int_{\mathbb{R}} \mathbf{a}_p f \mathrm{d}\mathbf{c}$, the break-up disappearance terms $\mathscr{B}^{n_p -} = \nu_p n_p$ and $\mathscr{B}^{u_d -} = \nu_p n_p \mathbf{u}_p$ and the break-up creation terms:

$$\begin{array}{ll} \mathscr{B}^{n_d p+} = R_p \displaystyle\int_{\mathbb{R}} \nu_d n_d(\xi') b_p(\xi', \xi) \mathrm{d}\xi' & \mathscr{B}^{u_d p+} = R_p \displaystyle\int_{\mathbb{R}} \nu_d n_d(\xi') b_p(\xi', \xi) \mathbf{u}_p^{\mathrm{B}}\big(\xi', \mathbf{u}_d(\xi')\big) \mathrm{d}\xi' \\ \mathscr{B}^{n_l l+} = \nu_l \chi_\alpha \boldsymbol{D}_\xi^\alpha n_l(\xi) + K_2 \dfrac{\partial n_l}{\partial \xi}(\xi) & \mathscr{B}^{u_l l+} = \nu_l \chi_\alpha \boldsymbol{D}_\xi^\alpha (n_l \mathbf{u}_l)(\xi) + K_2 \dfrac{\partial n_l \mathbf{u}_l}{\partial \xi}(\xi) \end{array} \tag{4.4}$$

4.2. *Size discretization: the multi-fluid model*

The phase space of the semi-kinetic system has too high a dimension and requires therefore further modeling. So we move to the Eulerian Multi-Fluid (MF) model (Massot *et al.* 2009). The MF method has already been used for break-up modeling with presumed NDFs by Dufour *et al.* (2003); Doisneau *et al.* (2013); Doisneau (2013). We choose two discretizations $-\infty = \xi_{p,0} < \xi_{p,1} < \cdots < \xi_{p,N_p} = \infty$ for the droplet and ligament size phase spaces and we average the conservation law systems (4.2) and (4.3) over each fixed size interval $\mathscr{S}_{p,k} = [\xi_{p,k-1}, \xi_{p,k}[$, called sections. The set of droplets or ligaments in one section can be seen as a "fluid" for which conservation equation are written, the sections exchanging mass and momentum. Some size moments are considered, the number of which increases accuracy and cost. In our case and as an illustration, we choose to conserve number and mass $(n_{p,k}\ ,\ m_{p,k}) = \int_{\mathscr{S}_{p,k}} \big(1,\ \rho_{\mathrm{l}} \mathcal{V}_p(\xi)\big) n_p \mathrm{d}\xi$ which corresponds to the Two-Size Moment method, proven to be efficient in industrial simulations with strong droplet distribution variations, e.g., due to coalescence (Doisneau *et al.* 2012; Doisneau 2013). The following size distribution forms are also presumed:

$$n_p(\xi) = \sum_{k=1}^{N_p} \kappa_{p,k}(\xi) \mathbf{1}_{\mathscr{S}_{p,k}}(\xi), \tag{4.5}$$

corresponding to assume in each section a different form for n_p as a function of ξ (e.g., piecewise linear functions), a different velocity $\mathbf{u}_{p,k}$ as constant of ξ, and eventually a different shape to define $\mathcal{V}_p(\xi)$, $\mathrm{Surf}_p(\xi)$, etc.. We finally get conservation equations with source terms for droplets and ligaments of section k:

$$\left\{\begin{array}{ll} \partial_t n_{d,k} + \partial_{\mathbf{x}} \cdot (n_{d,k} \mathbf{u}_{d,k}) & = -\mathscr{B}_k^{n_d -} + \mathscr{B}_k^{n_d d+} + \mathscr{C}_k^{n_l d+} \\ \partial_t m_{d,k} + \partial_{\mathbf{x}} \cdot (m_{d,k} \mathbf{u}_{d,k}) & = -\mathscr{B}_k^{m_d -} + \mathscr{B}_k^{m_d d+} + \mathscr{C}_k^{m_l d+} \\ \partial_t (m_{d,k} \mathbf{u}_{d,k}) + \partial_{\mathbf{x}} \cdot (m_{d,k} \mathbf{u}_{d,k} \otimes \mathbf{u}_{d,k}) & = -\mathscr{B}_k^{u_d -} + \mathscr{B}_k^{u_d d+} + \mathscr{C}_k^{u_l d+} + m_{d,k} \overline{\mathbf{a}}_{d,k} \end{array}\right. \tag{4.6}$$

$$\begin{cases} \partial_t n_{l,k} + \partial_{\mathbf{x}}\cdot(n_{l,k}\mathbf{u}_{l,k}) & = \mathscr{B}_k^{n_d l+} - \mathscr{B}_k^{n_l -} + \mathscr{B}_k^{n_l l+} - \mathscr{C}_k^{n_l d-} \\ \partial_t m_{l,k} + \partial_{\mathbf{x}}\cdot(m_{l,k}\mathbf{u}_{l,k}) & = \mathscr{B}_k^{m_d l+} - \mathscr{B}_k^{m_l -} + \mathscr{B}_k^{m_l l+} - \mathscr{C}_k^{m_l d-} \\ \partial_t(m_{l,k}\mathbf{u}_{l,k}) + \partial_{\mathbf{x}}\cdot(m_{l,k}\mathbf{u}_{l,k}\otimes\mathbf{u}_{l,k}) & = \mathscr{B}_k^{u_d l+} - \mathscr{B}_k^{u_l -} + \mathscr{B}_k^{u_l l+} - \mathscr{C}_k^{u_l d-} + m_{l,k}\overline{\mathbf{a}}_{l,k} \end{cases} \tag{4.7}$$

where the drag terms are $m_{p,k}\overline{\mathbf{a}}_{p,k} = \int_{\mathscr{S}_{p,k}} \rho_\mathrm{l}\mathcal{V}_p(\xi)\kappa_{p,k}(\xi)\overline{\mathbf{a}}_p \mathrm{d}\xi$, the disappearance terms are:

$$\begin{pmatrix} \mathscr{B}^{n_p -} \\ \mathscr{B}_k^{m_p -} \\ \mathscr{B}_k^{u_p -} \end{pmatrix} = \int_{\mathscr{S}_{p,k}} \nu_p \begin{pmatrix} 1 \\ \rho_\mathrm{l}\mathcal{V}_p(\xi) \\ \rho_\mathrm{l}\mathcal{V}_p(\xi)\mathbf{u}_{p,k} \end{pmatrix} \kappa_{p,k}(\xi)\mathrm{d}\xi \tag{4.8}$$

the discrete creation terms see the inner integral decomposed (Dufour *et al.* 2003):

$$\begin{pmatrix} \mathscr{B}_k^{n_d p+} \\ \mathscr{B}_k^{m_d p+} \\ \mathscr{B}_k^{u_d p+} \end{pmatrix} = \int_{\mathscr{S}_{p,k}} R_p \sum_{i=1}^{N_d} \int_{\mathscr{S}_{d,i}} \nu_d \begin{pmatrix} 1 \\ \rho_\mathrm{l}\mathcal{V}_d(\xi) \\ \rho_\mathrm{l}\mathcal{V}_d(\xi)\mathbf{u}_p^\mathrm{B}(\xi', \mathbf{u}_{d,i}) \end{pmatrix} \kappa_{d,i}(\xi') b_p(\xi', \xi)\mathrm{d}\xi'\mathrm{d}\xi \tag{4.9}$$

and the ligament continuous creation terms are integrals:

$$\begin{pmatrix} \mathscr{B}_k^{n_l l+} \\ \mathscr{B}_k^{m_l l+} \\ \mathscr{B}_k^{u_l l+} \end{pmatrix} = \int_{\mathscr{S}_{l,k}} \nu_l \chi_\alpha \begin{pmatrix} \boldsymbol{D}_\xi^\alpha n_l(\xi) \\ \rho_\mathrm{l}\mathcal{V}_l(\xi)\boldsymbol{D}_\xi^\alpha n_l(\xi) \\ \rho_\mathrm{l}\mathcal{V}_l(\xi)\boldsymbol{D}_\xi^\alpha n_l(\xi)\mathbf{u}_{l,k} \end{pmatrix} \mathrm{d}\xi + \int_{\mathscr{S}_{l,k}} K_2 \begin{pmatrix} \partial_\xi n_l(\xi) \\ \rho_\mathrm{l}\mathcal{V}_l(\xi)\partial_\xi n_l \\ \rho_\mathrm{l}\mathcal{V}_l(\xi)\partial_\xi n_l \mathbf{u}_{l,k} \end{pmatrix} \mathrm{d}\xi \tag{4.10}$$

of first order size derivatives (on the right in (4.10)) that are computed as evaporation terms ,i.e., they become fluxes from/to neighbor sections (Kah 2010) and of fractional derivatives which are in fact integro-differential operators which couple all sections. The overall system is therefore closed and can be computed with methods from the literature.

Acknowledgment

The authors acknowledge CTR for their hospitality and their financial support. The support of the France-Stanford Center for Interdisciplinary Studies through a collaborative project grant (P. Moin/M. Massot) is gratefully acknowledged as well.

REFERENCES

Amsden, A. A., O'Rourke, P. J. & Butler, T. D. 1989 Kiva II, a computer program for chemically reactive flows with sprays. *Tech. Rep.* LA-11560-MS. Los Alamos National Laboratory, Los Alamos, New Mexico.

Apte, S., Mahesh, K., Moin, P. & Oefelein, J. 2003 Large-eddy simulation of swirling particle-laden flows in a coaxial-jet combustor. *Int. J. of Multiphase Flows* **29** (8), 1311 – 1331.

Doisneau, F. 2013 Eulerian modeling and simulation of polydisperse, moderately dense, coalescing spray flows with nanometric-to-inertial droplets: application to Solid Rocket Motors. PhD thesis, Ecole Centrale Paris.

Doisneau, F., Laurent, F., Murrone, A., Dupays, J. & Massot, M. 2012 Eulerian Multi-Fluid models for the simulation of dynamics and coalescence of particles in solid propellant combustion. *To appear in J. Comp. Physics* pp. 1–37.

Doisneau, F., Montreuil, E., Dupays, J., Murrone, A. & Laurent, F. Secondary break-up in aerospace with CEDRE. *In prep. for Int. J. of Multiphase Flows*

Dufour, G., Massot, M. & Villedieu, P. 2003 Study of a secondary break-up model for sprays. *C. R. Math. Acad. Sci. Paris* **336** (5), 447–452.

Eggers, J. & Villermaux, E. 2008 Physics of liquid jets. *Reports on Progress in Physics* **71**, 036601.

Fox, R. 2012 Large-Eddy-Simulation tools for Multiphase Flows. *Annu. Rev. Fluid Mech.* **44**, 47–76.

Gorenflo, R., Mainardi, F., Moretti, F., Pagini, G. & Paradisi, P. 2002 Discrete random walks models for space-time fractional diffusion. *J. Chem. Phys.* **284**, 521–541.

Gorokhovski, M. & Herrmann, M. 2008 Modeling primary atomization. *Annu. Rev. Fluid Mech.* **40**, 343–366.

Gorokhovski, M. & Saveliev, V. 2003 Analyses of Kolmogorov's model of break-up et its application into Lagrangian computation of liquid sprays under air-blast atomization. *Phys. Fluid.* **15**, 184.

Hsiang, L.-P. & Faeth, G. 1995 Drop deformation and break-up due to shock wave and steady disturbance. *Int. J. Multiphase Flow* **21**, 545–560.

Kah, D. 2010 Taking into account polydispersity for the modeling of liquid fuel injection in internal combustion engines. PhD thesis, Ecole Centrale Paris.

Kolmogorov, A. 1941 On the logarithmically normal law of distribution of the size of particles under pulverization. *Dokl. Akad. Nauk. SSSR* **31**, 99.

Le Chenadec, V. 2012 Development of a Robust and Conservative Framework for Primary Atomization Computations. PhD thesis, Center for Turbulence Research, Stanford University.

Lefebvre, H. 1989 *Atomization and Sprays*. Hemisphere Publishing Corporation.

Massot, M., Laurent, F., de Chaisemartin, S., Fréret, L. & Kah, D. 2009 Eulerian Multi-Fluid models: modeling and numerical methods. In *Model. and Computation of Nanoparticles in Fluid Flows*, *Lect. von Karman Institute* 1, 1–86.

Novikov, E. & Dommermuth, D. 1997 Distribution of droplets in a turbulent spray. *Phys. Rev. E.* **56**, 5479.

Pilch, M. & Erdman, C. 1987 Use of break-up time data and velocity history data to predict the maximum size of stable fragments for acceleration-induced breakup of a liquid drop. *Int. J. Multiphase Flow* **13**, 741–757.

Rimbert, N. 2010 Simple model for turbulence intermittencies based on self-avoiding random vortex stretching. *Phys. Rev. E* **81**, 056315.

Rimbert, N. & Castanet, G. 2011 Crossover between Rayleigh-Taylor instability and turbulent cascading atomization mechanism in the bag-break-up regime. *Phys. Rev. E* **84**, 016318.

Rimbert, N. & Séro-Guillaume, O. 2004*a* Fragmentation equation and Riesz-Feller diffusion between scales. In *1st IFAC workshop on fractional differentiation and its application FDA04 (Bordeaux, France)*

Rimbert, N. & Séro-Guillaume, O. 2004*b* Log-Stable laws as asymptotic solutions to a fragmentation equation: application to the distribution of droplets in a high Weber number spray. *Phys. Rev. E.* **69**, 056316.

Williams, F. A. 1958 Spray combustion and atomization. *Phys. Fluids* **1**, 541–545.

Zhao, H., Liu, H., Li, W. & Xu, J. 2010 Morphological classification of low viscosity drop bag break-up in a continuous air jet stream. *Phys. Fluids* **22**, 114103.

Ziff, R. & McGrady, E. 1987 Shattering transition in Fragmentation. *Phys. Rev. Lett.* **58**, 892–895.